CERN-TH/98-249
hep-ph/9807570

A new approach to multi-jet calculations in hadron collisions [1]

F. Caravaglios[a], M.L. Mangano[a] [2], M. Moretti[a,b] and R. Pittau[a]

[a] CERN, Theoretical Physics Division,
CH 1211 Geneva 23, Switzerland

[b] Dept. of Physics and INFN, Ferrara, Italy

Abstract

We present an algorithm to evaluate the exact, tree-level matrix elements for multi-parton processes in QCD. We tested this technique, based on the recursive evaluation of the S-matrix, on processes such as $gg \to n$ gluons and $q\bar{q} \to n$ gluons, with n up to 9. The summation over colour configurations is designed to allow the construction of parton-level event generators suitable to interfacing with a parton-shower evolution including the effects of colour-coherence. This leads to a fully exclusive, hadron-level description of multi-jet final states, accurately incorporating the dynamics of large jet-jet separation angles. Explicit results for the total rates and differential distributions of processes with 8 final-state partons are given.

CERN-TH/98-249
August 1998

[1] This work was supported in part by the EU Fourth Framework Programme "Training and Mobility of Researchers", Network "Quantum Chromodynamics and the Deep Structure of Elementary Particles", contract FMRX–CT98–0194 (DG 12 – MIHT).

[2] On leave of absence from INFN, Sezione di Pisa, Italy.

1 Introduction

Multi-jet final states play an important role in the study of high-energy collisions. They provide in fact interesting signatures for several phenomena, both within the Standard Model (e.g. top-pair production), and beyond it (e.g. multi-jet decays of supersymmetric particles such as gluinos and squarks). The accurate determination of the properties of these phenomena requires a good understanding of the properties of the usually large multi-jet QCD backgrounds, which can distort the shapes of signal distributions and affect the measurement of quantities such as resonances' masses. In the past few years, several theoretical developments have allowed the calculation of very complicated multi-parton processes in QCD (for a review, see [1]) [3]. For example, the complete set of leading-order (LO) background processes to the production and decay of top-quark pairs in hadronic collisions is known for both the fully hadronic decays [2], and the $e\nu$+4-jet decays [3].

While significant progress has been made in the field of one-loop corrections (for a review see [4]), quantitative studies of multi-jet processes (with $n > 3$) can only be done today using tree-level results, which are the subject of the present work. There are several reasons for wanting to improve the tools currently available to perform these calculations.

1. First of all, interesting final states with larger jet multiplicities will become available with the next generation of colliders (LHC and NLC). This will hold both for standard QCD processes, where the huge available phase-space will allow production of many high-E_T jets, and for potential signals of new physics (a good example being cascade decays of heavy squarks or gluinos with R-parity non-conservation, where final states with over 10 jets would be a typical signature). This calls for improved algorithms, to allow the calculation of cross-sections for complicated processes within reasonable amounts of computer time.

2. Secondly, one would like to be able to complement the calculation of parton-level matrix elements with the evaluation of the full hadronic structure of the final state. This is a key ingredient for a satisfactory study of both signal and background components and for a complete comparison between theory and data. It involves the consistent merging of the matrix-element computation with the parton-shower evolution, a problem which has not been considered in the development of previous tools for the evaluation of multi-jet processes.

While relations are known [5] which allow to systematically evaluate high-order tree-level processes in a recursive fashion, the complexity of the algorithm grows very quickly and makes progress beyond the processes listed above very hard. Several approximations have therefore been introduced [6, 7], to evaluate with rather low computing time and acceptable accuracy cross-sections for many partons in the final state. Nevertheless, the knowledge of the exact parton level matrix elements will always be needed, in order to assess the reliability of the approximations used.

In this work we present an approach to the calculation of tree-level matrix elements for multi-parton final states which addresses both of the above problems, and therefore improves on the currently available algorithms. The key element of this proposal is the use of the algorithm `ALPHA`, developed by two of us [8] for the evaluation of arbitrary multi-parton matrix elements. This algorithm determines the matrix elements from a (numerical) Legendre transform of the effective

[3] We shall include under the label QCD also all processes with the emission of electro-weak gauge bosons, such as associated production of W's and jets.

Process	$n=7$	$n=8$	$n=9$	$n=10$
$g\ g \to n\ g$	559,405	10,525,900	224,449,225	5,348,843,500
$q\bar{q} \to n\ g$	231,280	4,016,775	79,603,720	1,773,172,275

Table 1: Number of Feynman diagrams corresponding to amplitudes with different numbers of quarks and gluons.

action, using a recursive procedure which does not make explicit use of Feynman diagrams. The algorithm has a complexity growing like a power in the number of particles, compared to the factorial-like growth that one expects from naive diagram counting. This is a necessary feature of any attempt to evaluate matrix elements for processes with large numbers of external particles, since the number of Feynman diagrams grows very quickly beyond any reasonable value. For example, the number of tree-level Feynamn diagrams corresponding to a process with n_g gluons and n_q pairs of quarks (with $n_q = 0, 1$), is given by the following formula [4]:

$$N_{diag} \;=\; \left[\left(y\frac{\partial}{\partial x} + xy^3\frac{\partial}{\partial y} + z^2 y\frac{\partial}{\partial z}\right)^{n_g+2n_q-3} \quad x^{1-n_q}\, y^{3-2n_q}\, z^{2n_q}\right]_{x=y=z=1} \tag{1}$$

A similar formula can be constructed for processes with more than 1 quark pair. The number of diagrams relevant for some of the examples considered in this paper are collected in Table 1. These numbers clearly illustrate the problems encountered when trying to evaluate the amplitudes by calculating each individual diagram, whether by algebraic or by numerical means.

`ALPHA` has been shown to operate very successfully in the case of purely electroweak processes [9], and will be reviewed here in Section 2. Its application to the case of QCD, although straightforward, requires some care due to the rapid increase of the number of colour configurations with the number of external coloured particles. Furthermore, the choice of how to organise the sum over colour structures has important implications for the possibility to merge the evaluation of a given matrix element with the successive parton-shower QCD evolution. Several options are available, in principle, to deal with the summation over all possible colour configurations. They will be discussed in Section 3, where our strategy for an efficient generation of Monte-Carlo events, combined with the possibility to generate colour configurations suitable for a parton-shower evolution, will be presented. Some numerical examples of applications of this tecnique to the case of $2 \to 8$ parton processes in hadronic collisions are given in Section 4. A more complete study, including the treatment of associated production of jets and electroweak gauge bosons and the description of a complete event generator interfaced to a parton-shower program such as `HERWIG` [10], will be presented in the future.

[4] The formula can be easily derived as follows. For a given diagram consider the triplet (p, q, g), where p is the number of 3-gluon vertices, q is the total number of external quark legs and internal quark propagators, and g is the total number of gluonic external legs and internal propagators. The number of diagrams obtained by attaching an additional gluon in all allowed ways is given by: p diagrams of type $(p-1, q, g+1)$, plus q diagrams of type $(p, q+1, g+1)$ plus g diagrams of type $(p+1, q, g+2)$. These triplets can be obtained by applying the operator $y\partial/\partial x + xy^3\partial/\partial y + z^2 y\partial/\partial z$ to the function $x^p\, y^g\, z^q$. Their multiplicities are given by the coefficients of the relative monomials, and the total number of generated diagrams is extracted by setting $x = y = z = 1$ in the polynomial thus obtained. Repeated iteration of this operator on the three-point diagrams ggg and $q\bar{q}g$, represented by the monomials $x\, y^3$ and $y\, z^2$, gives the desired result.

Independently of our efforts, work by Draggiotis, Kleiss and Papadopoulos [11] has recently addressed the problem of the efficient generation of multi-parton QCD final states using the ALPHA algorithm. In this work they turn the summation over colours into an integration over a continuous set of variables, slightly gaining in computational accuracy over the more standard colour-summation technique presented in our work. The integration technique, however, does not lend itself in an obvious way to the efficient merging of the parton-level calculation with the parton-shower evolution. In either case, it is quite clear that improvements in the numerical efficiency of these calculations will be possible, and work should be devoted in the future to find the best compromise among all different requirements to be met for a faithful and efficient representation of these highly complex processes.

2 The ALPHA algorithm

In reference [8], a new approach to the computation of tree level scattering amplitudes was introduced. This approach, based on the numerical Legendre transform of the effective action, is particularly useful for the automatic calculation of multi-particle processes. This technique was implemented in a Fortran code [8] which has been succesfully used to study several intricated electroweak processes [9]. For the sake of completeness, we review in this Section the ALPHA algorithm; the interested reader can find a more detailed discussion in the original paper [8], which includes an explicit analytic example for the $\lambda\phi^3$ theory.

Let Γ be the one-particle-irreducible generator of the Green functions for a given theory. Then the computation of the S-matrix requires the evaluation of the Legendre transform, Z, of Γ:

$$Z(J^\alpha) = -\Gamma(\phi^\alpha) + J^\alpha(x)\phi^\alpha(x) \tag{2}$$

where ϕ^α are the classical fields defined as the solutions of

$$J^\alpha = \frac{\delta\Gamma}{\delta\phi^\alpha} \,, \tag{3}$$

and the J^α play the role of classical sources. In general the Lagrangian contains several fields, with different spin and internal quantum numbers. It may also contain interactions with an arbitrary number of fields; for our purposes it is better to rearrange the Lagrangian into an equivalent form which includes only trilinear interactions: this can be achieved by introducing a proper set of auxiliary fields[5]. The Lagrangian in momentum space is

$$\begin{aligned}\mathcal{L} &= \frac{1}{2}\int d^4\bar{p}\; d^4\bar{q}\; \bar{\delta}(p+q)\; \tilde{\Pi}^{\alpha\beta}(p^2)\; \phi^\alpha(p)\; \phi^\beta(q) + \\ &+ \frac{1}{6}\int d^4\bar{p}\; d^4\bar{q}\; d^4\bar{k}\; \bar{\delta}(p+q+k)\; \phi^\alpha(p)\; \phi^\beta(q)\; \phi^\gamma(k)\; \mathcal{O}^{\alpha\beta\gamma}(p,q,k) \,,\end{aligned}$$

where the greek indices are a compact notation for Lorentz indices, internal symmetry indices, flavour etc. and where $d^4\bar{p} = d^4p/(2\pi)^4$ and $\bar{\delta} = (2\pi)^4\delta^4$. $\tilde{\Pi}^{\alpha\beta}(p^2)$ is the inverse propagator and $\mathcal{O}^{\alpha\beta\gamma}(p,q,k)$ is a generic function of the momenta. In the case of translationally invariant

[5]For example a term of the type $\lambda\phi^4$ can be replaced by the equivalent form $\lambda\phi^2 X - 1/4X^2$, where X is an auxiliary field. The equation of motion for the auxiliary field, $X = 2\lambda\phi^2$, makes this equivalence manifest.

local interactions $\mathcal{O}$ is a polynomial in the momenta. To obtain the connected Green function $G^{\alpha\beta\cdots\gamma}(p_1 \cdots p_n)$ from the above Lagrangian we introduce the classical sources

$$J^\alpha(q) = \sum_{i=1}^{n} a_i^\alpha \bar{\delta}(q - p_i) \tag{4}$$

where the a_i^α carry the same quantum numbers as the source J^α. With this choice of the J^α the amplitude $\mathcal{A}$ is given by[6]:

$$\mathcal{A} = \frac{\partial Z}{\partial a_1^\alpha \ldots \partial a_n^\gamma}|_{a_1^\alpha = 0, \ldots, a_n^\gamma = 0} \tag{5}$$

The equations of motion of eq. (3) can be written as

$$\phi^\alpha(q) = \tilde{\Pi}^{-1}_{\alpha\lambda}(q) \left[J^\lambda(q) - \frac{1}{2} \int d^4\bar{p}\; d^4\bar{k}\; \bar{\delta}(q + k + p)\; \phi^\beta(k)\; \phi^\gamma(p)\; \mathcal{O}^{\lambda\beta\gamma}(q, k, p) \right]. \tag{6}$$

It is clear that this equation for $\phi(q)$ can be solved perturbatively with respect to the interaction $\mathcal{O}^{\alpha\beta\gamma}$ (or, equivalently, with respect to the a_i^α) and the $(t+1)$-th order of this perturbative series is obtained by inserting the expansion of the $\phi^\alpha(q)$ up to the t-th order in the right-hand side of eq. (6). To recover the functional derivative of eq. (5) and avoid unnecessary computations it is useful to introduce the prescription to drop out terms which contain powers of the a_j^α larger than one, at any iteration step. With this prescription, using the initial condition (4) and the recursive relation (6), we can prove by induction that the solution $\phi^\alpha(q)$ is of the form

$$\phi^\alpha(q) = \sum_{j=1}^{2^n - 2} b_j^\alpha\; \bar{\delta}(q - P_j) \tag{7}$$

with

$$P_j = c_j^i\; p_i \qquad\qquad c_j^i = 0, 1. \tag{8}$$

Here an important point should be noticed: the Lagrangian $\mathcal{L}$ of eq. (4) is reduced to a simple function of a finite number of b_j^α variables, by means of eq. (4) with the constraint given in eq. (8). Namely, plugging the explicit expressions of eq. (7) into the Lagrangian of eq. (4) we obtain

$$\begin{aligned} \mathcal{L} \;&=\; \frac{1}{2} \int\; d^4\bar{p}\; d^4\bar{q}\; \bar{\delta}(p + q)\; \tilde{\Pi}^{\alpha\beta}(P_j^2)\; \bar{\delta}(p - P_j)\; \bar{\delta}(q - P_r)\, b_j^\alpha\; b_r^\beta + \\ &+\; \frac{1}{6} \int d^4\bar{p}\; d^4\bar{q}\; d^4\bar{k}\; \bar{\delta}(p + q + k)\; \mathcal{O}^{\alpha\beta\gamma}(p, q, k)\; \bar{\delta}(p - P_j)\; \bar{\delta}(q - P_r)\; \bar{\delta}(k - P_t)\; b_j^\alpha\; b_r^\beta\; b_t^\gamma \end{aligned} \tag{9}$$

We define the matrices

$$\Delta_{jl}^{\alpha\beta} = \int d^4\bar{p}\; d^4\bar{q}\; \bar{\delta}(p + q)\; \tilde{\Pi}^{\alpha\beta}(P_j^2)\; \bar{\delta}(p - P_j)\; \bar{\delta}(q - P_l) \tag{10}$$

and

$$D_{jlm}^{\alpha\beta\gamma} = \int d^4\bar{p}\; d^4\bar{q}\; d^4\bar{k}\; \bar{\delta}(p + q + k)\; \mathcal{O}^{\alpha\beta\gamma}(p, q, k)\; \bar{\delta}(p - P_j)\; \bar{\delta}(q - P_l)\; \bar{\delta}(k - P_m). \tag{11}$$

[6]For the sake of simplicity, we omit from this expression the explicit truncation of the external propagators.

After integration they become:

$$D^{\alpha\beta\gamma}_{jlm} = \begin{cases} \mathcal{O}^{\alpha\beta\gamma}(P_j, P_l, P_m) & \text{if} \quad P_j + P_l + P_m = 0 \\ \\ 0 & \text{if} \quad P_j + P_l + P_m \neq 0 \end{cases} \tag{12}$$

$$\Delta^{\alpha\beta}_{jl} = \begin{cases} \tilde{\Pi}^{\alpha\beta}(P_j^2) & \text{if} \quad P_j + P_l = 0 \\ \\ 0 & \text{if} \quad P_j + P_l \neq 0. \end{cases} \tag{13}$$

We recall that, in the above expressions, $\mathcal{O}^{\alpha\beta\gamma}$ is the interaction in momentum space, $\tilde{\Pi}^{\alpha\beta}$ is the inverse propagator and the quantities D_{jlm} and Δ_{jl} satisfy the four-momentum conservation by construction.

The function Z then becomes

$$Z = a_i^\alpha b_i^\alpha - \frac{1}{2}\, b_j^\alpha\, b_l^\beta\, \Delta^{\alpha\beta}_{jl} \; - \; \frac{1}{6}\, b_j^\alpha\, b_l^\beta\, b_m^\gamma\, D^{\alpha\beta\gamma}_{jlm}. \tag{14}$$

Equation (6) provides us with a set of iterative relations for the b_j^α: after the substitution in eq. (7), and performing the integrals over the momenta, we are left with a relation which gives us each b_j at the order t ($b_{j,t}$) in the interaction coefficient $\mathcal{O}$, in terms of the $b_{j,r}$ (with $r < t$)[7]

Namely, we have [8]

$$\begin{aligned} b^\alpha_{j,0} &= a^\alpha_j \quad j = 1, n \\ b^\alpha_{j,0} &= 0 \quad j > n \qquad n\text{= number of external particles} \\ b^\alpha_{j,1} &= -\frac{1}{2}(\Delta^{-1})^{\alpha\beta}_{j,m}\, D^{\beta\gamma\delta}_{m,k,l} \sum_{l\neq k} b^\gamma_{k,0} b^\delta_{l,0} \\ &\vdots \qquad\quad \vdots \\ b^\alpha_{j,t} &= -\frac{1}{2}(\Delta^{-1})^{\alpha\beta}_{j,m}\, D^{\beta\gamma\delta}_{m,k,l} \sum_{r+s=t-1} b^\gamma_{k,r}\, b^\delta_{l,s} \end{aligned} \tag{15}$$

where the condition $l \neq k$ derives from the constraint in eq. (8). The full scattering amplitude is recovered by plugging $b_j^\alpha = \sum_t b_{j,t}$ in eq. (14) and keeping only terms which are proportional to $a_1^\alpha a_2^\beta \cdots a_n^\gamma$ (the only ones that contribute to the limit $a \to 0$)

$$\mathcal{A}_{p_1,\ldots,p_n} = -\frac{1}{2} \sum_{s+r=n-2} b^\alpha_{j,r}\; \Delta^{\alpha\beta}_{j,l} b^\beta_{l,s} - \frac{1}{6} \sum_{s+r+t=n-3} D^{\beta\gamma\delta}_{j,k,l}\; b^\beta_{j,r}\; b^\gamma_{k,s}\; b^\delta_{l,t} + b^\alpha_{j,n-2}\; a^\beta_l\; \tilde{\Pi}^{\alpha\beta}_{j,l}. \tag{16}$$

Notice that in eqs. (14)–(16) repeated indices are summed over, in particular repeated latin indices are summed from 1 to $2^n - 2$, namely over the non-zero momenta contributing to eq. (7).

Equation (16) can be further simplified using the equations of motion. The solution b_j to $\partial Z/\partial b_j = 0$, has been found for any value of the expansion parameter, thus the minimization is satisfied order by order in the perturbative expansion, *i.e.* $\partial Z/\partial b_{j,t} = 0$. For simplicity, let us discuss the case of an odd number of particles n. It is easy to check by inspection that each term in eq. (16) can contain at most one $b_{j,t}$ with $t > n/2 - 1$. Therefore we can reorganize eq. (16) by

[7] In the following j, k, l, m will always label quantities that are in one to one correspondence with the momenta P_j in eq. (7), whereas r, s, t will denote the order of the perturbative expansion.

collecting each $b_{j,t}$ with $t > n/2-1$. The coefficients of these terms cannot depend on other $b_{j,t'}$ with $t' > n/2-1$ (they are only polynomial in $b_{j,\bar{t}}$ with $\bar{t} < n/2-1$) and therefore we can simply drop such terms from eq. (16). The above simplification also applies to the case of even n, and it amounts to keeping only the trilinear terms in eq. (16) and limiting the summation to a subset of the b_j^α [8]. Then, an additional restriction on the quantities c_j^i in eq. (8) is obtained:

$$\mathcal{A}_{p_1,\ldots,p_n} \;=\; -\frac{1}{6}\sum_{j,k,l\in\mathcal{P}}\sum_{s+r+t=n-3} \mathcal{O}^{\beta\gamma\delta}_{j,k,l}\; b^\beta_{j,r}\; b^\gamma_{k,s}\; b^\delta_{l,t}\;, \tag{17}$$

with:

$$j\in\mathcal{P} \quad \text{if} \quad \left\{ \begin{array}{c} \sum_i c_j^i < n/2 \\ \text{or} \\ \sum_i c_j^i = n/2, \quad \text{with} \;\; c_j^1 = 1\,. \end{array} \right. \tag{18}$$

A final remark is in order here. In eqs. (15) one has to take properly into account Bose/Fermi statistics. Formally this can be achieved by introducing a set of Grassman variables ϵ_j, so that $\epsilon_j\epsilon_k+\epsilon_k\epsilon_j = 0$, and setting $u(p) \to \epsilon u(p)$ for the fermion sources, where $u(p)$ is a vector of ordinary numbers. In practice this means that each term in the sums of eqs. (15) enters with a relative sign, depending on the order of the b_j.

The advantage of the iterative eqs. (15) is that they can now be easily implemented in a `Fortran` code. Note that the recursive relations have been obtained for a completely generic Lagrangian, without using any specific property of the interaction (*e.g.* identities on the structure constants of SU(3), or the Lorentz structure of the interaction etc.). With this algorithm we can thus compute the scattering amplitude for any physical initial and final states. In particular, any colour structure can be assigned to the external legs (while for example the Berends-Giele's recursive relations [15] have only been derived for colour-ordered amplitudes) and weak bosons (as well as other particles beyond the Standard Model) can be incorporated. Finally, the algorithm has an exponential growth of the CPU time with the number of external particles (instead of a factorial growth) and it can take into account the particle masses without increasing the computing time.

As a final remark, we point out that the algorithm presented above can be further optimised in the specific case of the QCD Lagrangian. In fact the pure Yang-Mills Lagrangian

$$\mathcal{L}_{YM} = -\frac{1}{4}F^a_{\mu\nu}F^a_{\mu\nu} \tag{19}$$

can be rewritten as

$$\mathcal{L}_{YM} = -\frac{1}{2}B^a_{\mu\nu}B^a_{\mu\nu} + \frac{1}{4}B^a_{\mu\nu}F^a_{\mu\nu} \tag{20}$$

This form of the Lagrangian has the virtue that a single interaction term of the form BAA is left, instead of the two interaction terms which are present in eq. (19). This saves CPU time when performing the iteration step given in eq. (15). A further reduction in the algorithm complexity can be obtained by using the Coulomb gauge $A^a_0 = 0$, which reduces the number of components of the field A^a_μ from four to three and those of the field $B^a_{\mu\nu}$ from six to three.

3 Summing over colours

The proper bookkeeping of the colour structure of QCD processes has been one of the main ingredients in the simplification of the calculations of multi-parton processes in QCD which took

place in the past years. It has been shown [12] that by expanding the matrix element for a given QCD process in a particular colour basis, the coefficients of each colour structure in this basis enjoy important properties which make their calculation much simpler. As an example, the scattering amplitude for n gluons with momenta p_i^μ, helicities ϵ_i^μ and colours a_i (with $i = 1, \ldots, n$), can be written as:

$$M(\{p_i\}, \{\epsilon_i\}, \{a_i\}) \;=\; \sum_{P(2,3,\ldots,n)} \mathrm{tr}(\lambda^{a_1}\,\lambda^{a_2}\ldots\lambda^{a_n})\; A(1,2,\ldots,n)\;. \tag{21}$$

The sum extends over all permutations P of $(2, 3, \ldots, n)$, and the functions $A(1, 2, \ldots, n)$ (known as *dual* or *colour-ordered* amplitudes) are gauge-invariant, cyclically-symmetric functions of the gluons' momenta and helicities[8]. All of the colour-dependence is absorbed in the trace coefficients, and the dual amplitudes are colour-independent. In these special bases some particular helicity amplitudes [14] have very simple analitical expressions [12, 5], regardless of the number of external partons, and all amplitudes obey recursive relations [5] which make it possible to numerically evaluate them systematically for arbitrarily complex processes [16, 15, 13]. Thanks to additional properties of these functions, only $(n-2)!$ of them are truly independent, and the remaining ones can be obtained from specific *linear* combinations [13].

Furthermore, when summing over colours the amplitude squared, different orderings of dual amplitudes are orthogonal at the leading order in $1/N^2$:

$$\sum_{\mathrm{col's}} |M(\{p_i\}, \{\epsilon_i\}, \{a_i\})|^2 \;=\; N^{n-2}(N^2-1) \sum_{P(2,3,\ldots,n)} \left[|A(1,2,\ldots,n)|^2 + \frac{1}{N^2}(\mathrm{interf.}) \right]\;. \tag{22}$$

It is therefore possible to achieve an accuracy to leading-order in $1/N^2$ by neglecting the evaluation of the subleading interferences, reducing significantly the complexity of the numerical evaluations.

Similar expansions hold for processes involving one [17, 5] or more [18] quark pairs. In the case of amplitudes with one quark pair, for example, one has the following expansion:

$$M(q_\alpha, \bar{q}_\beta, \{p_i\}, \{\epsilon_i\}, \{a_i\}) \;=\; \sum_{P(1,2,\ldots,n)} (\lambda^{a_1}\,\lambda^{a_2}\ldots\lambda^{a_n})_{\alpha\beta}\; A(q, \bar{q}, 1, 2, \ldots, n) \tag{23}$$

where the gauge-invariant functions $A(q, \bar{q}, 1, 2, \ldots, n)$ obey remarkable properties similar to those of the gluonic amplitudes.

Dual amplitudes can be easily evaluated using the `ALPHA` algorithm. Since the dual amplitudes A are independent of the number of colours, they can be calculated exactly by taking N sufficiently large. Considering for example the case of an n-gluon amplitude, we can choose $N > n$ and select the following set of λ matrices to represent the gluon colours $a_1, \ldots, a_n$:

$$(\lambda^{a_i})_{jk} \;=\; \frac{1}{\sqrt{2}}\delta_{i,j}\delta_{i+1,k} \quad (i = 1, \ldots, n-1) \qquad , \quad (\lambda^{a_n})_{jk} \;=\; \frac{1}{\sqrt{2}}\delta_{n,j}\delta_{k,1} \tag{24}$$

With this colour choice the dual amplitude corresponding to the permutation $(1, 2, \ldots, n)$ is proportional to the full amplitude, as the only non-vanishing colour factor in eq. (21) is

$$\mathrm{tr}(\lambda^{a_1}\lambda^{a_2}\ldots\lambda^{a_n}) \;=\; \frac{1}{2^{n/2}}\;. \tag{25}$$

[8] For simplicity we will just use the indices $i = 1, \ldots, n$, as opposed to using the full symbols p_i and ϵ_i, to specify the relevant permutation of momenta and helicities.

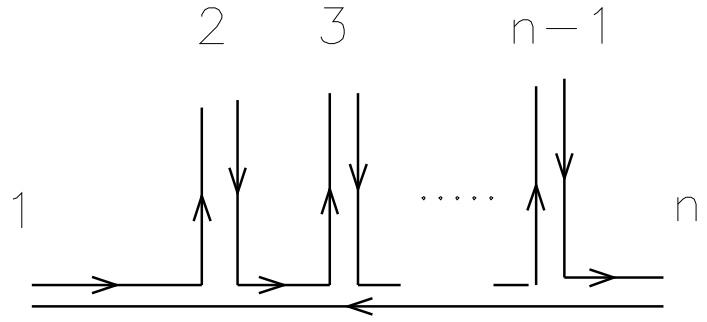

Figure 1: Colour structure of the n-gluon amplitude in the large-N limit.

We explicitly calculated multi-gluon dual amplitudes using the large-N colour-matrices given in eq. (24). We verified the correctness of the calculation for n up to 11 by comparing the results for maximally helicity violating (MHV) amplitudes [14] (e.g. $g^+g^+ \to g^+ \cdots g^+$) with the analytic expressions known exactly for arbitrary n [12, 5]. The input of the numerical evaluation of the matrix element is a string containing the total number of gluons, their helicity state, and their momenta. From these data, the amplitude is evaluated automatically. Since the evaluation performed with the `ALPHA` algorithm does not treat the case of MHV amplitudes differently than any other helicity combination, and since we checked the numerical calculation using several different gauges (which allowed us to ensure that no accidental cancellation of individual diagrams takes place), we are confident that our code correctly evaluates the dual amplitudes for arbitrary helicity configurations. We extended this test to processes with one and two $q\bar{q}$ pairs, where analytic expressions are known for similar MHV amplitudes [1], and found perfect agreement.

The use of dual amplitudes for the evaluation of multi-parton processes has one valuable feature, and one serious drawback. The valuable feature is the fact that dual amplitudes admit a simple physical interpretation, which as we shall show makes them the required starting point for the parton-shower evolution of the parton-level process. The serious drawback is that their number grows factorially with n, so that while each individual dual amplitude can be easily and quickly calculated, using the technique given above, the number of dual-amplitude calculations which are necessary to get the full matrix element squared and summed over colours becomes soon too large to be practical. In the rest of this Section we will first explain in more detail the role of dual amplitudes for the parton-shower evolution of the hard process, and then present a way to bypass the rapid growth of their multiplicity.

Dual amplitudes correspond to planar amplitudes in the $N \to \infty$ limit of QCD. At large N, the colour structure given by the assignement in eq. (24) corresponds to having the colour flowing from gluon 1 to gluon 2, from gluon 2 to gluon 3, and so on, until the colour of the last gluon flows back to gluon 1 (see fig. 1). The identification of a specific colour flow makes it possible to incorporate soft-gluon emission corrections to the hard process. In fact the soft-gluon emission probability from a planar amplitude is given, in the large-N limit, by the incoherent sum over the emission probabilities from each individual colour-string [19, 12, 15]. In the case of a multi-gluon amplitude, for example, we get:

$$\sum_{\text{col's}} |M(p_1,\ldots,p_n,k)|^2 \overset{k\to 0}{\to} g^2 N \sum_{P(1,2,\ldots,n)} \sum_{i=1,\ldots,n} \frac{(p_i \cdot p_{i+1})}{(p_i \cdot k)\,(p_{i+1} \cdot k)}\, |A(1,2,\ldots,n)|^2 + \mathcal{O}(1/N^2)\,, \tag{26}$$

where $n+1$ and 1 are identified in the above equation. Inclusion of soft-gluon virtual corrections

factorises in a similar fashion, and Sudakov form factors for the soft-gluon emission probability can be defined, to next-to-leading logarithmic accuracy, to describe the parton-shower evolution from any such colour-ordered process [19, 10]. Perfectly similar equations can be written in the case of processes involving quark pairs.

The prescription to correctly generate the parton-shower associated to a given event in the large-N limit is therefore the following:

1. Calculate the $(n-1)!$ dual amplitudes corresponding to all possible planar colour configurations.

2. Extract the *most likely* colour configuration for this event on a statistical basis, according to the relative contribution of the single configurations to the total event weight [9]. Since each dual amplitude is gauge invariant, the choice of colour-configurations is also a gauge-invariant operation.

3. Develop the parton shower out of each initial and final-state parton, starting from the selected colour configuration. This step can be carried out by feeding the generated event to a Monte-Carlo program such as `HERWIG`, which is precisely designed to *turn partons into jets* starting from an assigned colour-ordered configuration.

Notice that, if the dual amplitudes are evaluated for a specific helicity configuration, `HERWIG` will also include spin-correlation effects in the evolution of the parton shower [20, 10].

With the physical value of $N = 3$, dual amplitudes corresponding to different permutations will however interfere with each other, as shown in eq. (22). This interference is suppressed by powers of $1/N^2$ [17], as well as by dynamical factors: for example, the behaviour of interference terms is less singular near collinear or soft momentum configurations than the leading terms in N. Within the $1/N^2$ approximation which is employed in the description of coherence effects in the shower evolution [10], it is therefore consistent to neglect the interferences between different dual amplitudes for the selection of the colour structure to be assigned to a given event. After calculating the total weight of a given event, accurate to all orders in $1/N$, we can thus still use the procedure described in point 2 above to assign a definite colour configuration to the event itself.

As a result, use of the dual-amplitude representation of a multi-gluon amplitude allows to accurately describe not only the large-angle correlations in multi-jet final states, but also the full shower evolution of the initial- and final-state partons with the same accuracy available in `HERWIG` for the description of 2-jet final states.

In the $N \to \infty$ limit the choice of the dual amplitude basis has also one important advantage. Since interferences between different colour structures vanish in this limit, one can perform the sum over colours by Monte-Carlo methods. Rather than evaluating the full matrix element squared, summed over all colour structures, one can randomly select a dual colour structure on an event-by-event basis, and just evaluate the corresponding contribution to the amplitude squared. An overall multiplicative coefficient proportional to the number of dual colour configurations provides the correct normalization. Assuming that, on average, all colour configurations contribute the same amount to the cross-section, this approach is numerically more efficient than summing each

[9] Defining $w_i = |A_i|^2$ for each colour flow i, and $W_i = \sum_{k=1,\dots,i} w_k \,/\, \sum_{k=1,\dots,n} w_k$, the j-th colour structure will be selected if $W_{j-1} \leq \xi < W_j$, for a random number ξ uniformly distributed over the interval $[0,1]$.

event over all colours. Furthermore, one could optimise the selection of colour configurations, to adapt it to possible differences in their individual overall contributions. This is similar to what is usually done to perform the sum over quark and gluon helicities.

At finite N this procedure is not applicable anymore, as interferences between various colour structures do not vanish. At the same time, the matrix describing all possible colour interferences has a size growing like $[(n-1)!]^2$, which makes its storing and access highly inefficient.

We propose to solve this problem as follows. First of all we choose the following orthonormal basis for the Gell-Mann λ matrices:

$$\lambda^1 = \frac{1}{\sqrt{2}}\begin{pmatrix} 0 & 1 & 0 \\ 0 & 0 & 0 \\ 0 & 0 & 0 \end{pmatrix} \quad , \quad \lambda^2 = \frac{1}{\sqrt{2}}\begin{pmatrix} 0 & 0 & 1 \\ 0 & 0 & 0 \\ 0 & 0 & 0 \end{pmatrix} \quad , \quad \lambda^3 = \frac{1}{\sqrt{2}}\begin{pmatrix} 0 & 0 & 0 \\ 1 & 0 & 0 \\ 0 & 0 & 0 \end{pmatrix}$$

$$\lambda^5 = \frac{1}{\sqrt{2}}\begin{pmatrix} 0 & 0 & 0 \\ 0 & 0 & 1 \\ 0 & 0 & 0 \end{pmatrix} \quad , \quad \lambda^6 = \frac{1}{\sqrt{2}}\begin{pmatrix} 0 & 0 & 0 \\ 0 & 0 & 0 \\ 1 & 0 & 0 \end{pmatrix} \quad , \quad \lambda^7 = \frac{1}{\sqrt{2}}\begin{pmatrix} 0 & 0 & 0 \\ 0 & 0 & 0 \\ 0 & 1 & 0 \end{pmatrix}$$

$$\lambda^4 = \frac{1}{2}\begin{pmatrix} 1 & 0 & 0 \\ 0 & -1 & 0 \\ 0 & 0 & 0 \end{pmatrix} \quad , \quad \lambda^8 = \frac{1}{\sqrt{12}}\begin{pmatrix} 1 & 0 & 0 \\ 0 & 1 & 0 \\ 0 & 0 & -2 \end{pmatrix}$$

In this basis, only a fraction of all possible 8^n colour assignements gives rise to a non-zero amplitude. For each event, we randomly select a non-vanishing colour assignement for the exernal gluons, and evaluate the amplitude M. The weight of the event is proportional to $|M|^2$, multiplied by the number of non-zero colour configurations. This is all we need if we are not interested in evolving the event with the parton shower. If instead we want to generate the parton shower, we first decide, with standard unweighting techniques, whether to accept the event. If the event is accepted, we list all dual amplitudes contributing to the chosen colour configuration according to eq. (21) and, among these dual amplitudes, we randomly select a colour flow on the basis of their relative weight[10].

In a 6-gluon amplitude, for example, a possible non-zero colour assignement is given by $(2,7,5,6,1,3)$. Up to cyclic permutations, only three orderings of the colour indices give rise to non-vanishing traces: $\mathrm{tr}(\lambda^2\,\lambda^7\,\lambda^5\,\lambda^6\,\lambda^1\,\lambda^3)$, $\mathrm{tr}(\lambda^2\,\lambda^6\,\lambda^1\,\lambda^5\,\lambda^7\,\lambda^3)$ and $\mathrm{tr}(\lambda^2\,\lambda^7\,\lambda^3\,\lambda^1\,\lambda^5\,\lambda^6)$. Therefore only three dual amplitudes contribute to the full amplitude: $A(2,7,5,6,1,3)$, $A(2,6,1,5,7,3)$ and $A(2,7,3,1,5,6)$. The colour ordering to be specified for the coherent parton-shower evolution can be selected by comparing the size of the squares of $\mathrm{tr}(\lambda^2\,\lambda^{i_2}\ldots\lambda^{i_6})\,A(2,i_2,\ldots,i_6)$ for the three contributing permutations $(i_2,\ldots,i_6)$ of the colour indices.

Since the average number of dual amplitudes involved in the evaluation of a single element of the orthogonal basis is smaller than $(n-1)!$, the complexity of the procedure grows more slowly than for the calculation done using directly the dual basis. The distribution of the number of dual amplitudes contributing to all possible colour assignements in the orthogonal basis for $n = 8, 9$ and 10 gluons is shown in fig. 2. Furthermore, considering that only unweighted events are usually evolved by the parton shower, and that unweighted events are a small fraction of all generated parton-level events, the decomposition in terms of dual amplitudes only needs to be performed for a small fraction of the generated configurations.

[10] We explicitly checked the numerical implementation of this algorithm by comparing our results for the colour-summed squared amplitudes of the $gg \to \mathrm{n}\,g$ and $q\bar{q} \to \mathrm{n}\,g$ processes (for $n = 4, 5$) with the known results obtained in ref. [13], as implemented in the `NJETS` code [2]. The agreement is at the level of machine precision.

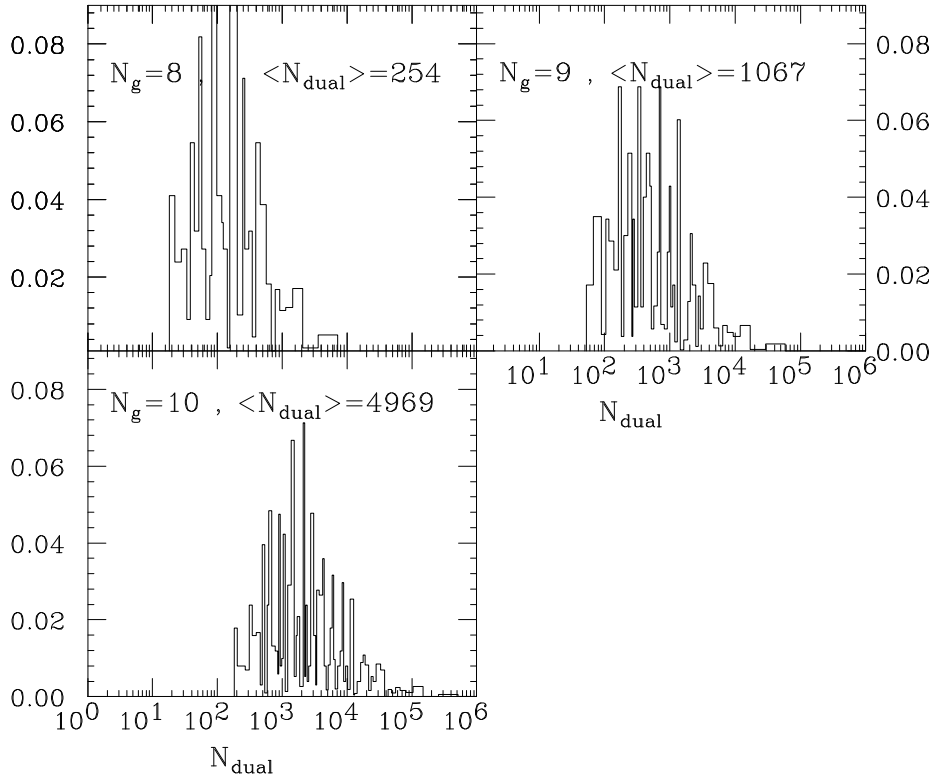

Figure 2: Distribution of the number of dual amplitudes contributing to all possible colour assignements in the orthogonal basis for $n = 8, 9$ and 10 gluons.

The results we present in the following are all relative to parton-level results, and therefore only the Monte-Carlo summation over orthogonal colour configurations is considered.

4 Results

As an example of our technique, we present here results for the following two parton-level processes:

$$\begin{aligned} g\ g &\to 8\ g \\ q\ \bar{q} &\to 8\ g\,. \end{aligned} \tag{27}$$

For comparisons, we also computed the above reactions in the simple approximation first suggested by Kunszt and Stirling [6]. This approximation (hereafter referred to as `SPHEL`) consists in assuming that the average value of MHV amplitudes is equal to the average value of all other non-zero amplitudes. In the case of n-gluon amplitudes this amounts to estimating the sum over all helicity configurations using the relation:

$$\sum_{\text{hel's}} \left|M\left(gg \to (\mathrm{n}-2)\, g\right)\right|^2 \;=\; \frac{2^n - 2(n+1)}{n(n-1)} \sum_{\text{MHV}} \left|M\left(gg \to (\mathrm{n}-2)\, g\right)\right|^2 \tag{28}$$

where the sum on the right-hand side runs over all MHV amplitues (e.g. $++ \to +\ldots+$, $+- \to -+\ldots+$, etc.). Their value is known exactly for all n at the leading-order in $1/N$ [14]:

$$\sum_{\text{MHV}} \left|M\left(gg \to (\mathrm{n}-2)\, g\right)\right|^2 \;=\; 4\left(\frac{g^2 N}{2}\right)^{n-2} (N^2-1) \sum_{i,j} (p_i \cdot p_j)^4$$

Process	Exact (pb)	SPHEL (pb)
$g\ g \to 8\ g$	0.719 ± 0.019	1.53 ± 0.03
$q\ \bar{q} \to 8\ g$	$(\,0.901 \pm 0.009\,)\times 10^{-3}$	$(\,1.042 \pm 0.008\,)\times 10^{-3}$

Table 2: Partonic cross-sections in pb at $\sqrt{\hat{s}} = 1500$ GeV, with the cuts described in the text.

$$\sum_{P(1,n-1)} \frac{1}{(p_1\cdot p_2)(p_2\cdot p_3)\cdots(p_n\cdot p_1)} \tag{29}$$

where the sum runs over all permutations $P(1,\ldots,n-1)$ of the indices $(1,\ldots,n-1)$. Similarly, in the case of $q\bar{q}g\ldots g$ amplitudes, the SPHEL approximation amounts to assuming:

$$\sum_{\text{hel's}} \left|M\left(q\bar{q}\to \text{n}\, g\right)\right|^2 \;=\; \frac{2^{n-1}-1}{n} \sum_{\text{MHV}} \left|M\left(q\bar{q}\to \text{n}\, g\right)\right|^2 \tag{30}$$

where the sum on the right-hand side runs over all MHV amplitues (e.g. $+-\to -+\ldots+$), whose value is known exactly for all n at the leading-order in $1/N$ [17]:

$$\begin{aligned}\sum_{\text{MHV}} \left|M\left(q\bar{q}\to \text{n}\, g\right)\right| \;=\; 4\left(\frac{g^2N}{2}\right)^n (N^2-1) \sum_{i=1,n} \Big[(p_q\cdot p_i)^3(p_{\bar{q}}\cdot p_i) + (p_q\cdot p_i)(p_{\bar{q}}\cdot p_i)^3\Big] \\ \frac{1}{p_q\cdot p_{\bar{q}}} \sum_{P(1,\ldots,n)} \frac{1}{(p_q\cdot p_1)(p_1\cdot p_2)\cdots(p_n\cdot p_{\bar{q}})}\,,\end{aligned} \tag{31}$$

where the sum runs over all permutations $P(1,\ldots,n)$ of the indices $(1,\ldots,n)$.

The kinematic configuration and the cut values used in our numerical examples are as follows:

$$\sqrt{\hat{s}} = 1500\,\text{GeV}\,, \quad p_{T_i} > 60\,\text{GeV}\,, \quad |\eta_i| < 2\,, \quad \Delta R_{ij} > 0.7\,. \tag{32}$$

These values, and the choice of a fixed strong coupling $\alpha_s = 0.12$, only serve for illustrative purposes. A more complete phenomenological analysis of production cross-sections and a comparison of exact and approximate expressions will be presented elsewhere.

The integration over the phase space allowed by the cuts was performed by Monte Carlo using both RAMBO [21], a flat phase space generator, and a multichannel approach [22]. Both integration strategies gave compatible and comparable efficiencies. The sum over helicity configurations was performed via a flat Monte Carlo generation. No attempt has been made to optimise this step. Some of the details of the numerical performance of the algorithm are given at the end of the Section.

In Table 2 we present our Monte Carlo estimate for the partonic cross-sections, together with the values obtained by using SPHEL. SPHEL overestimates by about a factor 2 the exact cross-section for the process $g\ g \to 8\ g$, while it is accurate at the 10% level for $q\ \bar{q} \to 8\ g$.

Notice the large ratio of the gg-initiated amplitude, relative to the $q\bar{q}$ one. In the case of $2\to 2$ processes, this ratio is of order 30 for a reference scattering angle $\theta = \pi/2$, while here it is much larger. It is easy to understand this result considering the structure of the MHV amplitudes in the

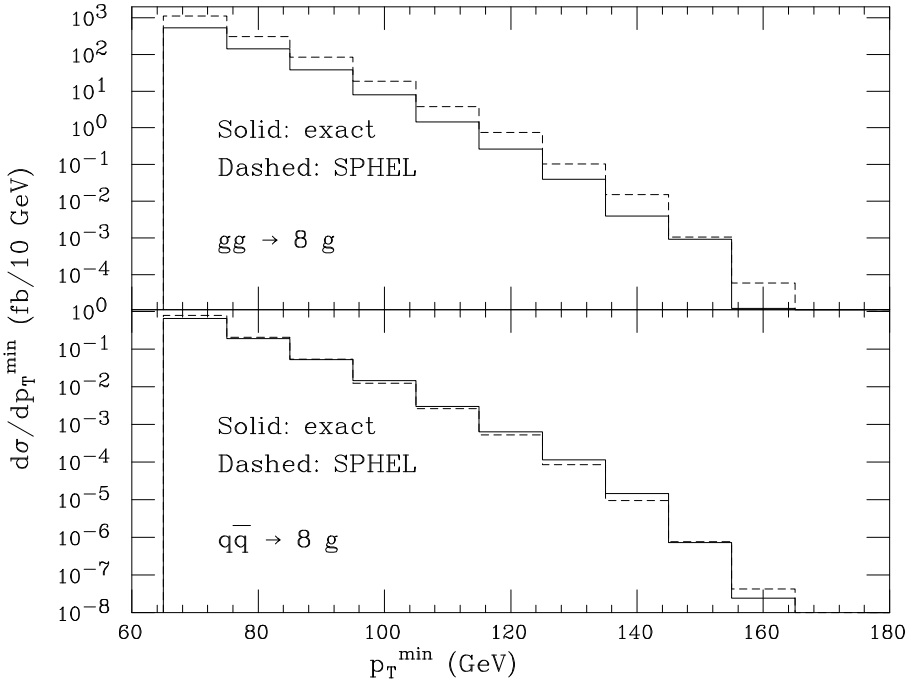

Figure 3: Differential distributions for the minimum gluon transverse momentum. Exact result vs. SPHEL.

two cases. In the gluon-only case, eq. (29), the numerators are dominated by the term $(p_1 p_2)^4 \sim \hat{s}^4$, while in the $q\bar{q}$ case, eq. (31), only terms proportional to t-channel momentum exchange appear. With the increase in the number of final-state particles, the average momentum exchanged in the t-channels becomes smaller, while $\hat{s}$ stays the same, and the ratio $\hat{s}/\langle t \rangle^4$ becomes very large.

We also considered differential cross-sections. In Fig. 3, we show the distribution of the minimum gluon transverse momentum for both processes. A good agreement between the exact and the SPHEL result is observed. Considering the large uncertainties present in the overall normalization of multi-parton tree-level processes (e.g. those induced by changes in the choice of the renormalization and factorization scales), the approximated evaluation can provide in many cases a sufficient description of the final-state distributions.

In Figs. 4 and 5 we plot the distributions for the maximum gluon transverse momentum and the maximum two-gluon invariant mass. Again there is a reasonable agreement between the exact and the approximated result, in particular in the case of the gluon-only process.

Before closing this Section, we present some technical details to illustrate the performance of the algorithms used to produce our results. As an example, consider the process $g\ g \to 8\ g$. As shown in Table 1, the total number of Feynman diagrams contributing to this process is 10,525,900. The plots in this work have been obtained from the evaluation of the matrix elements for 1.9×10^6 Monte Carlo points passing the selection cuts given in eq. (32) (out of 1.8×10^8 points selected by the phase-space generator). The efficiency for the generation of the non zero weights, defined as the average weight divided by the maximum weight, was about 1×10^{-4}. The computational time for producing 100 events that pass the cuts, with a 200 MHz processor [11], and working in double precision throughout, was about 91 seconds for the exact matrix element and 2.3 seconds using the SPHEL approximation. In this last case, the dominant component of the CPU budget is

[11] All of the following numbers are reduced by a factor of 4 when using a DEC Alpha station.

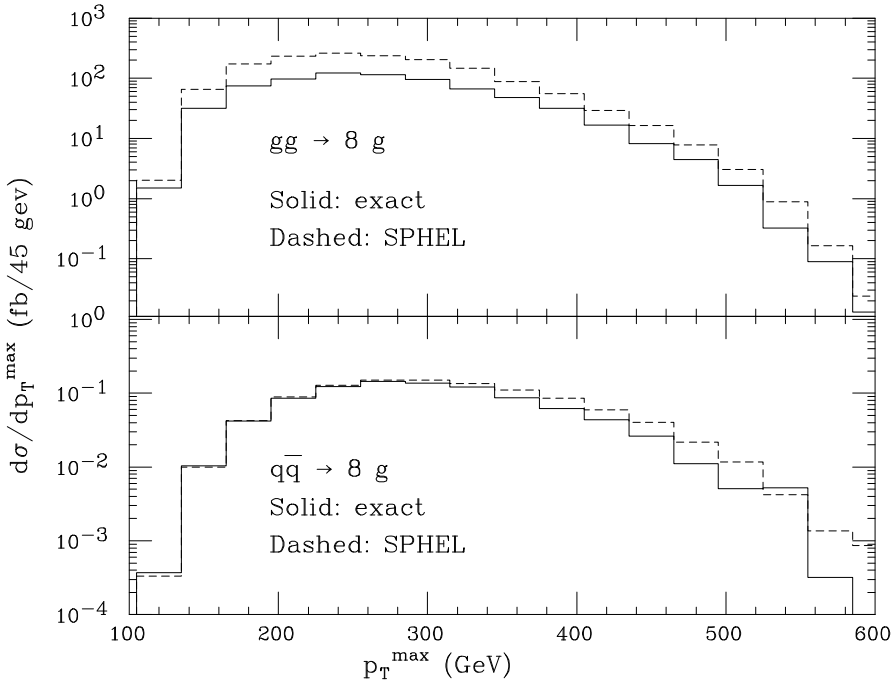

Figure 4: Differential distributions for the maximun gluon transverse momentum. Exact result vs. SPHEL.

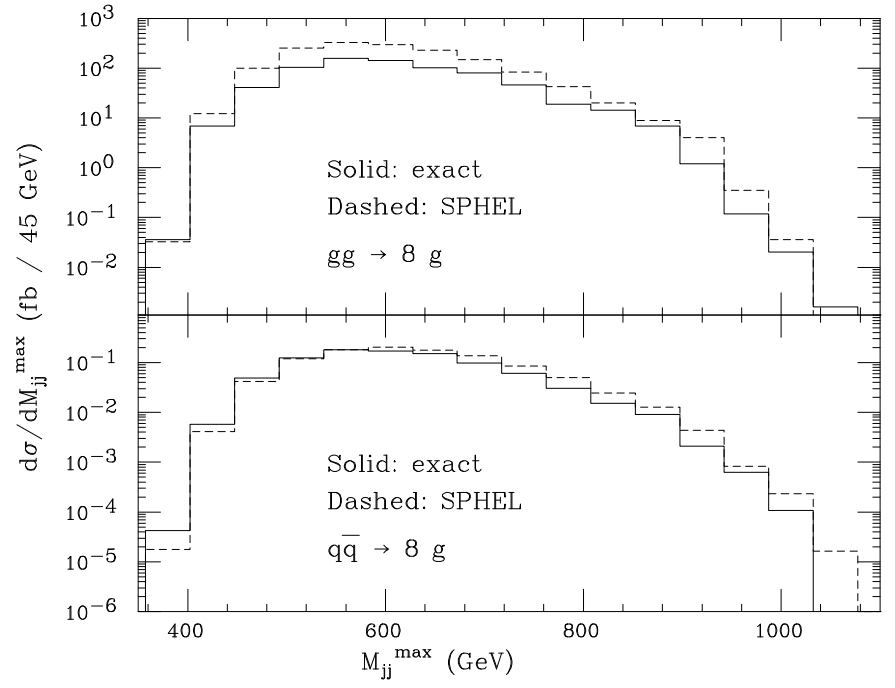

Figure 5: Differential distributions for the maximum two-gluon invariant mass. Exact result vs. SPHEL.

the search for phase-space configurations passing the selection cuts.

5 Conclusions

We presented in this work an algorithm to evaluate the exact, tree-level matrix elements for multi-parton processes in QCD. This technique, based on the algorithm `ALPHA`, has been tested for processes such as $gg \to n$ gluons and $q\bar{q} \to n$ gluons, with n up to 9. We discussed how the summation over colour configurations allows the construction of parton-level event generators suitable to interfacing with a parton-shower evolution including the effects of colour-coherence. This will eventually lead to a fully exclusive, hadron-level description of multi-jet final states, accurately incorporating the dynamics of large jet-jet separation angles.

While we confined our presentation to the case of hadroproduction, our program can be used without modifications for the evaluation of multi-parton production in e^+e^- collisions, since the relevant $SU(2) \times U(1)$ Lagrangian is already included in the code. Likewise, associated hadroproduction of gauge bosons and QCD partons is a straightforward application of our code.

We gave some explicit numerical results, considering parton-level cross-sections and distributions for the processes $gg \to 8$ gluons and $q\bar{q} \to 8$ gluons. We verified that some standard simple approximations to the multi-parton cross-sections provide a good description of the exact result, for both rates and distributions. The existence of the exact results allows now to extend the checks on these approximations to values of n larger than ever before. We expect that large improvements can be obtained in the numerical efficiency of the algorithm, and that cross-sections for up to 10 final-state partons should become feasible.

Furthermore, when n becomes so large that the evaluation of the exact amplitudes is numerically too slow for the generation of large samples of events, one can nevertheless use the approximated calculations to generate the samples, and lower statistics runs to assess the goodness of the approximation. In this respect, the numerical efficiency of the phase-space generation in presence of kinematic cuts will need to be improved as well.

Acknowledgements We thank P. Nason for useful discussions. The work of M. Moretti is funded by a Marie Curie fellowship (TMR-ERBFMBICT 971934).

References

[1] M.L. Mangano and S.J. Parke, Phys. Rep. **200** (1991) 301.
[2] F.A. Berends, W.T. Giele and H.Kuijf, Phys. Lett. **B232** (1989) 266.
[3] F.A. Berends, H.Kuijf, B. Tausk and W.T. Giele, Nucl. Phys. **B357** (1991) 32.
[4] Z. Bern, L. Dixon, D.A. Kosower, *Ann. Rev. Nucl. Part. Phys.* **46** (1996) 109.
[5] F.A. Berends and W.T. Giele, Nucl. Phys. **B306** (1988) 759.
[6] Z. Kunszt and W.J. Stirling, Phys. Rev. **D37** (1988) 2439.
[7] C.J. Maxwell, Phys. Lett. **B192** (1987) 190; Nucl. Phys. **B316** (1989) 321;
M.L. Mangano and S. Parke, Phys. Rev. **D39** (1989) 758.
[8] F. Caravaglios and M. Moretti, Phys. Lett. **B358** (1995) 332.

[9] F. Caravaglios and M. Moretti, Z. Phys. **C74** (1997) 291;
M. Moretti, Nucl. Phys. **B484** (1997) 3;
G. Montagna et al., *Eur.Phys.J.* **C2** (1998) 483.
[10] G. Marchesini and B.R. Webber, Nucl. Phys. **B310** (1988) 1161.
G. Marchesini, B.R. Webber, G. Abbiendi, I.G. Knowles, M.H. Seymour and L. Stanco, *Comp. Phys. Comm.* **67** (1992) 465.
[11] P. Draggiotis, R.H.P. Kleiss, C.G. Papadopoulos, CERN-TH/98-207, DEMO-HEP.98/01, `hep-ph/9807207`.
[12] M.L. Mangano, S.J. Parke and Z. Xu, Proceedings of Les Rencontres de Physique de la Vallee d'Aoste, (La Thuile, Italy, 1987), ed. M. Greco (Edition Frontieres), p.513.
F.A. Berends and W.T. Giele, Nucl. Phys. **B294** (1987) 700.
M.L. Mangano, S.J. Parke and Z. Xu, Nucl. Phys. **B298** (1988) 653.
[13] F.A. Berends, W.T. Giele and H.Kuijf, Nucl. Phys. **B333** (1990) 120.
[14] S.J. Parke and T. Taylor, Phys. Rev. Lett. **56** (1986) 2459.
[15] F.A. Berends and W.T. Giele, Nucl. Phys. **B313** (1989) 39.
[16] R. Kleiss and H. Kuijf, Nucl. Phys. **B312** (1989) 616.
[17] M.L. Mangano and S.J. Parke, Proceedings of Intern. Europhysics Conf. on High Energy Physics (Uppsala, sweden, 1987), ed. O. Botner, p.201.
M.L. Mangano and S.J. Parke, Nucl. Phys. **B299** (1988) 673.
[18] M.L. Mangano, Nucl. Phys. **B309** (1988) 461.
[19] A. Bassetto, M. Ciafaloni and G. Marchesini, Phys. Rep. **100** (1983) 201.
[20] J.C. Collins, Nucl. Phys. **B304** (1988) 794.
[21] W. J. Stirling, R. Kleiss and S. D. Ellis, Comput. Phys. Commun. **40** (1986) 359.
[22] R. Kleiss and R. Pittau, Comput. Phys. Commun. **83** (1994) 141.